AAS 20-511

THE BEHAVIOR OF HIGH-VELOCITY DUST GENERATED BY LANDER PLUMES IN THE LUNAR ENVIRONMENT

M.M. Wittal[*], J.R. Phillips III[†], P.T. Metzger[‡], B. Link [§], J.G. Mantovani[¶], D. Batcheldor [‖]

Lunar lander plumes are known to accelerate fine dust to speeds exceeding $2\,\mathrm{km\,s^{-1}}$, and the resultant ejecta may remain in lunar orbit for extended periods of time. Such ejecta could become hazardous to objects in lunar orbit as well as systems on the surface. In order to understand the impact on orbiting lunar infrastructure such as Gateway, as well as assets on the lunar surface, here we consider the dynamics of the resultant high-velocity plume ejecta. Initial conditions were set by the expected near-term lunar activity and the known cone of accelerated dust generated by previous lunar landings. The effects of regular 3-body gravitation, solar radiation pressure, and electric field are included in the model. It is found that although the majority of sub-μm dust is carried away by solar wind and electric fields, about $\sim$10 % of the dust between $1.7\,\mathrm{km\,s^{-1}}$ and $2.3\,\mathrm{km\,s^{-1}}$ reimpacts the surface, much of it near the landing site. The hazard posed by that debris is a function of lander mass and distance from the landing site. The Gateway, when orbiting in the nominal NRHO at the time of a landing, is not expected to be significantly affected by the dust. However, other spacecraft in less elliptic orbits may be at greater risk.

INTRODUCTION

Over billions of years, the process of bombardment and spallation from meteorites and larger bodies has created a lunar surface coated in regolith. This "impact gardening" has resulted in a size distribution in dust that averages about 70 μm and goes down to the sub-micron scale [1, 2]. In addition, this dust has been observed in a cloud around the moon that scatters sunlight [3, 4], and from impacts on orbiting spacecraft [5–7].

The impact of dust on lunar missions has long been a concern to spacecraft functionality, astronaut health, and general mission success [8]. The upcoming Artemis program and the return of humans to the Moon has renewed interest in understanding and mitigating the effects of lunar dust; however,

[*]NASA Kennedy Space Center (KSC) Granular Mechanics and Regolith Operations (GMRO) Laboratory & Gateway Logistics Service (GLS), NASA KSC Mail-code UB-E, Kennedy Space Center, FL 32899 & Embry-Riddle Aeronautical University, 600 S Clyde Morris Blvd, Daytona Beach, FL 32114

[†]NASA Kennedy Space Center (KSC) Electrostatics and Surface Physics Laboratory (ESPL), NASA KSC Mail-code UB-G, Kennedy Space Center, FL 32899

[‡]University of Central Florida Planetary Sciences Group, 4111 Libra Drive Physical Sciences Building (PSB) 430, Orlando, Florida 32816-2385

[§]SURA, LASSO-URS Federal Services Inc., Kennedy Space Center, FL 32899

[¶]NASA Kennedy Space Center (KSC) Granular Mechanics and Regolith Operations (GMRO) Laboratory, NASA KSC Mail-code UB-E, Kennedy Space Center, FL 32899

[‖]SURA, LASSO-URS Federal Services Inc., Kennedy Space Center, FL 32899

little attention has been paid to the behaviour of high-velocity dust generated by lander plumes, and its ultimate destination.

Predicting the destination of any given high velocity ($v > 2.2\,km\,s^{-1}$) particles is nontrivial in the 3-body system [9]. This problem is further complicated when considering the increased role of solar radiation pressure (SRP) and charge effects on very small particles (diameter < 1 mm). However, to assess the risks from ejecta created by regular landings to orbiting infrastructure such as the Gateway, as well as to surface operations, it is essential to understand the influences of these processes on the dynamics of lofted regolith.

Space Environment

In addition to the SRP, there are a number of other non-gravitational forces that could affect the dynamics of ejecta once above the lunar surface. The day-side of the Moon's surface is directly exposed to solar X-ray and UV photons, and the night-side of the Moon interacts with the lunar wake. The Earth-Moon system is embedded in the interplanetary magnetic field (IMF) and the solar wind. In addition, the Moon spends about 25 % of its orbit within the magnetospheric tail of Earth [10].

A net positive charging of the day-side lunar surface results from the solar X-ray and UV photoemission of electrons and the solar wind plasma. The net negative surface charging of the night-side results from enhanced electron temperatures in the lunar wake. The electric field, and the resultant dynamics of lunar dust, near the terminator is complex. The low altitude of the Sun, large shadows, and direct illumination of steep surfaces (crater rims, rocks) leads to complicated potentials due to localized electric field variations [11]. Consequently, charged particles near the lunar surface may experience a variety of electric-field-induced accelerations.

Away from the surface, the electromagnetic environment is dominated by the solar wind and Earth's magnetotail. Direct measurements of this environment over a 30-year period have shown an average magnetic field strength of 6.0 nT, a proton density of $6.7\,cm^{-3}$, plasma speed of $430\,km\,s^{-1}$, an electric field strength of $0.017\,mV\,m^{-1}$, and a solar flux of $1.1 \times 10^{-20}\,W\,m^2\,Hz^{-1}$, as extracted from NASA/GSFC's OMNI data set through OMNIWeb.

Dust Grain Charge

When in the plasma environment of the Earth's magnetotail, the electron number surface density present on dust grains near the lunar surface due may be estimated in the range of $10^{-4}\,\mu m^{-2}$ to $10^{-6}\,\mu m^{-2}$. These surface number densities correspond to surface charge densities of approximately $10^{-3}\,C\,m^{-2}$ to $10^{-1}\,C\,m^{-2}$ [12]. When outside Earth's magnetotail, and in the sunlit region of the lunar surface, dust grains will obtain surface charge densities much lower in magnitude. A conservative estimate of $10^{-6}\,C\,m^{-2}$ was therefore selected for use in these simulations. However, since capacitance increases with particle size, the approximation of a linear increase in charge with surface area will underestimate the charge for small particles and overestimate the charge for large particles. In addition, the current model does not account for additional charge accumulation due to triboelectric charge transfer between grains agitated during interaction of the plume with the lunar surface.

The lander will produce an environment similar to a fluidized particle bed frequently used in industry as the exhaust gases agitate and eject particles from the lunar surface. This type of process causes triboelectric charge transfer between interacting grains on the order of approximately

10^{-5} C m^{-2} due to the large number of energetic inter-particle contacts [13]. Additionally, charged particles within the exhaust plasma will accumulate on grains in the vicinity of the landing, further complicating the initial conditions. As such, these two additional sources of charge were neglected for the purposes of this investigation. Their inclusion in subsequent models will increase the effects seen on the particles interacting with the electromagnetic fields in the vicinity of the Moon.

METHOD

The trajectories of the particulates are simulated at the range of expected angles (azimuth and elevation) from the impingement point. These angles were determined by measuring the ejection angles of dust in the Apollo landing videos [14]. The initial velocities are described below. These initial trajectories were then numerically integrated over a long period of time considering various factors such as SRP, electric and magnetic fields of the Moon and space environment, and gravitational perturbations from the Earth, Moon, and Sun. As the size of such simulated particles decreases, the role of electromagnetic forces become increasingly influential as the cross-sectional area relative to particle masses is more significant. Thus, these forces are considered for each time step. Since simulating every dust particle generated by a lunar lander is impractical, each simulated particle is representative of the larger group.

Particle Size & Velocity Distribution

Previous work considered a total mass distribution based on a velocity when considering an impactor. However, for this work the ejected particles are the result of a rocket plume impingement, and treating that plume as an impactor would not produce an accurate result [15]. Instead, the ejected mass is treated purely as a function of lander mass:

$$M = 0.762 M_{\text{Lander}}^{1.77} \tag{1}$$

It is important to note that that M_{Lander} is in metric tonnes. This approximation may be used to gauge overall ejected mass, but does not provide a velocity distribution for that mass. Future work in developing Computational Fluid Dynamic (CFD) models will refine this approximation. For now, however, we turn to the model provided by [16] and [17], which is used to predict ejecta mass as a function of velocity.

Mass ejected above a given velocity can be estimated as:

$$dM(v) = C\left(v^{\frac{3\nu-1}{3\mu}}\right)^{-3\mu} \tag{2}$$

which is a simplification of the impactor formula provided by [16]. It can be simplified in this way because all we seek is the distribution of velocities and are applying a coefficient to match the displaced mass estimated by Eq. (2). The mass density exponent, ν, has been experimentally demonstrated to be 0.4, μ is the material-dependent exponent and will be estimated to be that of weakly cemented basalt, 0.55 [16], and C is the scaling coefficient which will be used to match $dM(1) = C = M$. Thus, by combining these formulae we get:

$$dM(v) = 0.762 M_{\text{Lander}}^{1.77}\left(v^{\frac{3\nu-1}{3\mu}}\right)^{-3\mu} \tag{3}$$

This estimate is combined with an estimated particle size distribution based on the diameters of the particles between 1 cm and 10 µm. This can then be used to approximate the average particle size at a given velocity, as well as the density of the particle cloud in the vicinity of the Moon.

CFD simulations have been performed for rocket exhaust under lunar landers, and individual particle trajectories calculated using Runge-Kutta numerical integration through the flow field [18]. The trajectory angles predicted by this method were in agreement with the ejecta angles measured in Apollo lander videos [14]. This numerical method also predicted the velocities of the particles as a function of their size, the distance from the centerline from which they were eroded, the lander thrust, and the lander height [18]. It was not possible to validate these velocity predictions for the fine sand-sized and dust-sized particles using the Apollo landing videos since such particles are not individually resolved in the videos. However, blown rocks were visible and their measured velocities [19] are in agreement with the simulations [18]. Together, the measured ejecta angles of the sand and dust, and the measured velocities of the rocks, provide a basic validation for the computer simulation method. NASA is currently performing an experimental campaign and developing lunar lander instruments to provide additional validation of the simulations, but for now we have used the best models that are available. The size-velocity distribution function predicted by [18] is summarized as:

$$N(r) = \frac{5 \times 10^5}{\tilde{N}(r)\left[12.5\left(10^6 r\right)^{1.4} + 0.0005\left(10^6 r\right)^{-5.2}\right]} \tag{4}$$

where the normalization factor $\tilde{N}$ can be defined as

$$\tilde{N}(r) = \int_{r_{\text{min}}}^{r_{\text{max}}} \left[12.5 r^{1.4} + 0.005 r^{-5.2}\right] dr \tag{5}$$

such that r is the radius in meters and N is the weighted number of particles. By discretizing this function into bins corresponding to each order of magnitude, converting the counts to mass, and summing the bins, we can determine how many of each sized particles are expected to be found in orbit.

SIMULATION

The primary simulation was performed using the FreeFlyer software, which is a tool for performing numerical integration of spacecraft and objects. FreeFlyer allows for the formation of constellations of spacecraft or, in this case, objects such as dust particles. Step size was constrained based on the anticipated position of Gateway in its orbit during the Artemis IV lunar landing. This gives Gateway the benefit of being able to avoid collision with most of the high-velocity dust that reimpacts the Moon within the first few days. However, some dust remains in orbit for much longer.

Dust Behavior in Orbit

EVD dust is most significantly influenced by lunar gravity. Direct LADEE/LDEX observations demonstrated a population of grains with radii of ∼0.3 µm ($q \geq 0.3$ fC) and ∼0.7 µm ($q \geq 4.0$ fC) at altitudes of up to 250 km with velocities on the order of a few hundred meters per second [7]. Assuming an average magnetic field strength of 8 nT, as observed by NASA's two Acceleration, Reconnection, Turbulence, and Electrodynamics of the Moon's Interaction with the Sun (ARTEMIS,

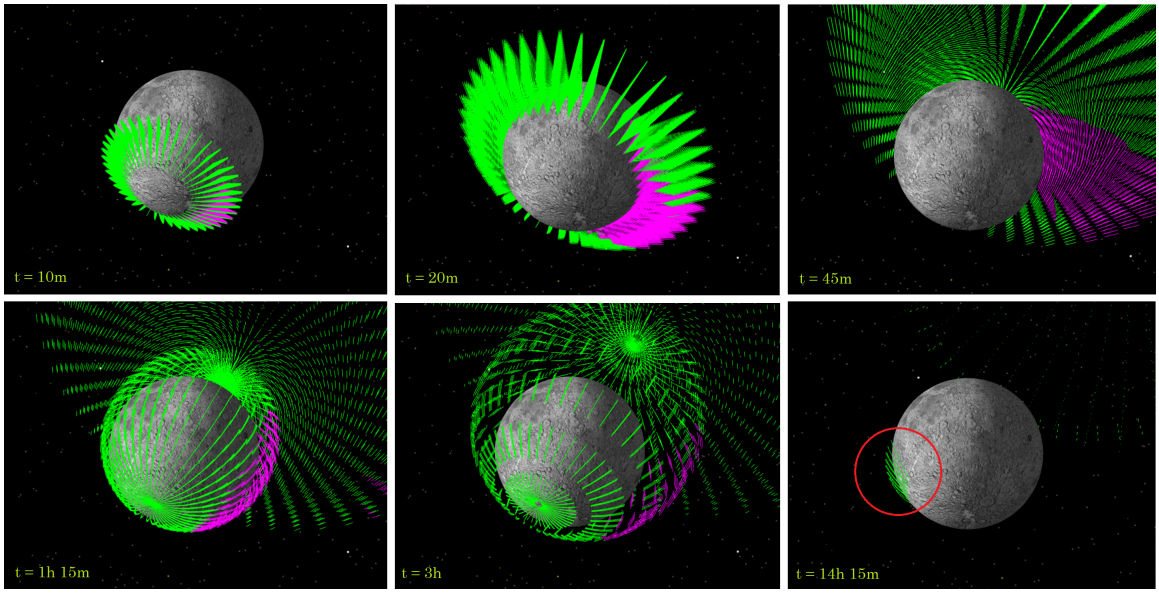

Figure 1. A visualization of the simulation over time. The purple locations indicate where the particles are in shadow and thus not effected by the solar wind. The red circle indicates a minority of particles that have begun orbiting in a trajectory that does not intersect the surface of the Moon.

different from the upcoming lunar south pole missions) spacecraft both in the direct solar wind and in Earth's magnetotail [20, 21], such a magnetic field could impart a force of up to 10^{-20} N. This is approximately 6-orders of magnitude less than the force due to lunar gravity. SRP, on the other hand, has a larger influence. For a solar constant of 1,400 W m^{-2} and a perfect absorber with a cross section of 10^{-12} m^2 ($\sim$0.7 µm radius), the force from SRP is approximately 3-orders of magnitude less than the force due to lunar gravity. This rapidly changes for smaller dust grains. For grains on the order of 1 nm, the forces from SRP and gravity are comparable.

However, lunar gravity falls off with the square of the distance, and many of the particles that would otherwise remain primarily under the influence of the Moon's gravity travel many thousands of kilometers away from the lunar surface before reimpacting the Moon or escaping to geocentric or heliocentric orbits [9].

At very low altitudes, however, the ejecta have become charged particles moving at a significant velocity through various electric fields. If these electric fields are larger than 13 V m^{-1} then a stationary 1 µm dust grain with a 10 V potential could levitate on the order of a meter above the surface [12], i.e., the electric force would be comparable to the gravitational force. However, at the lunar south pole the surface charging is complex as a result of its continuous proximity to the terminator, the constant proximity of the sun to the horizon, and a topology dominated by craters and other shadow-casting objects. Ejecta could therefore have a range of charges and travel through a range of electric fields. Nevertheless, the velocity of these ejecta minimizes the time spent in these fields. Therefore it is unlikely that lunar surface electric forces will result in any significant deviation to ejecta trajectories.

Particle Lifetimes

The standard lifetime of particles without considering charge averages 20 days, with some particles within the EVD lasting as much as 10 years in the lunar environment. For this work, the primary focus was the first 7 days. This period was chosen because the period of the nominal NRHO in which the Gateway will be placed is $\sim$6.5 days. Due to the extinction rate of the orbital dust, the density and thus the collision chance would be highest after the Gateway's first pass and would fall off exponentially after that.

Particle Diameter (mm)	Orbiting Particles (%)
10	5.8704
5	5.9074
1	6.0370
0.5	6.2963
0.1	7.9259
0.05	9.7037
0.01	19.1111

Table 1. The percentage of particles ejected at between 1.9 km s^{-1} and 2.3 km s^{-1} that remain in orbit after a period of 7 days.

Simulations were carried out to examine a variety of particle sizes from 10 mm to 10 µm and a velocity range of 1.7 km s^{-1} to 2.3 km s^{-1}. Each simulation had a total of 4,500 particles. At the end of the 7 days the status of each particle was assessed and it was revealed that the vast majority of particles had reimpacted the lunar surface, with a minority remaining in orbit. However, the amount that remained in orbit or escaped the lunar gravity well increased exponentially as particle size decreased, as seen in Fig. 2. This domain of particle size then remained the focus of the remained of the study.

RISK ASSESSMENT

By taking a large sample size of particles across the entire range of trajectories, a probability of reimpacting surface assets or damaging orbital infrastructure could be estimated. For this study, between 3,000 and 21,600 particles at a time were considered and observed over a period of 7 days, taking into consideration all of the physical effects described above.

For the purposes of the risk assessment, we must first determine the number of particles. First, we take Eq. (3) between the desired range of velocities, in our case 1.7 km s^{-1} to 2.3 km s^{-1}. This yields 594 kg of material ejected within this domain for 10 t lander. Then, using Eq. (4) we calculate the distribution of particles within the range simulated. Particles larger than 0.01 m are not expected to make it to this velocity in any significant quantity, while particles smaller than 10 µm are exponentially more likely to be carried away by solar wind and electrical forces, as demonstrated in Fig. 2. That leaves a total of 11.2 % total particles ejected within the simulated range remaining to pose a hazard after 7 days. Of that 11.2 %, only $\sim$9.5 % is still in orbit. Using our estimate of 594 kg, it can be estimated that 56.5 kg remain in orbit and 537.5 kg deposit on the surface.

Risk to Surface Assets

Overall, particles within the EVD tend to reimpact within $\sim$100 km of the landing site. Looking at Fig. 3.b, it can be seen that a closer examination of the distribution of those impacts show that

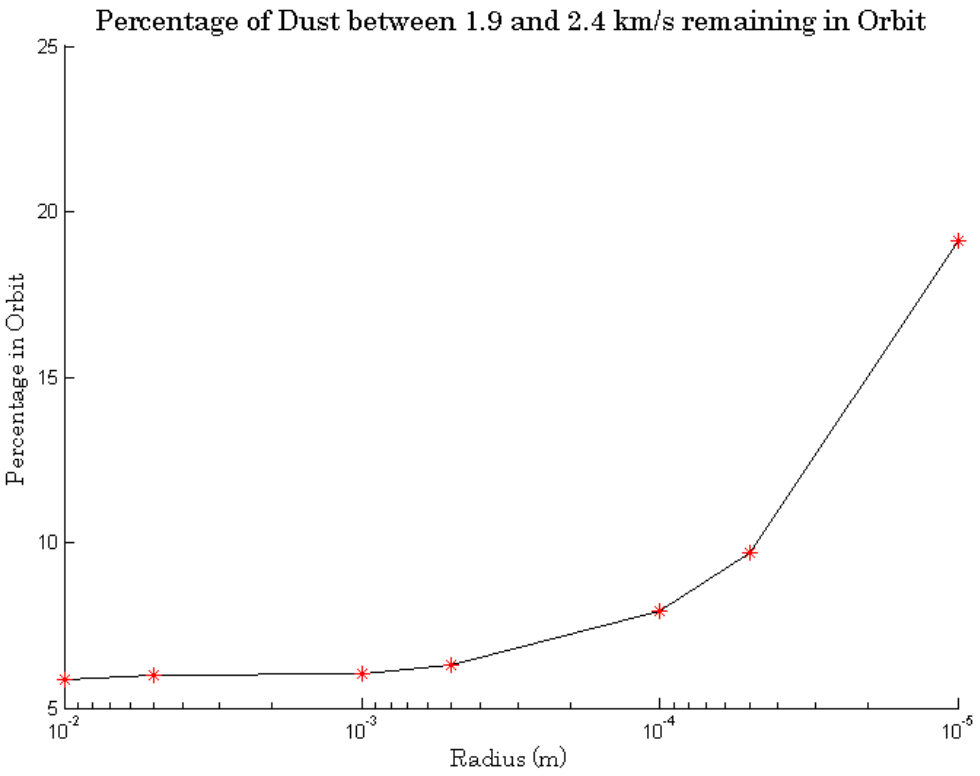

Figure 2. The percentage of particles ejected at between 1.9 km s^{-1} and 2.3 km s^{-1} that remain in orbit after a period of 7 days.

although the average distance from the landing site is roughly the same, the median reimpact of those particles increases relative to the landing site with respect to the departure speed. Higher speeds were not considered in this initial study due to the increased chance that the debris will escape. The chance of reimpacting lunar surface infrastructure significantly depends on their location relative to the landing site.

Since the amount of material that is redeposited has been determined above and the distribution is known as per Fig. 3, a risk assessment may be performed on surface assets as a function of area and distance from the landing site. Of the particles that reimpact the surface, the vast majority (greater than 99 %) are 10 µm or smaller in size. Thus, using the measured density of lunar regolith of 1,500 kg m^{-3}, and converting the 537.5 kg and the estimated 10 µm size of the deposited particles into a volume, it can be estimated that the deposited material consists of no fewer than ∼71,000 particles.

If spread uniformly over the lunar surface, the threat would be negligible. However, it is seen in Fig. 3.a that those deposits are more heavily concentrated near the landing site. By counting the number of impacts from the landing site, normalizing their distribution, and scaling it by 71,000, a radial distribution of impact density per unit area can be determined based on simulation results.

Thus, for an exposed lunar base occupying 1 km^2, the likelihood of sustaining an impact from a landing particle generated by 10 t lander may be described by the equation:

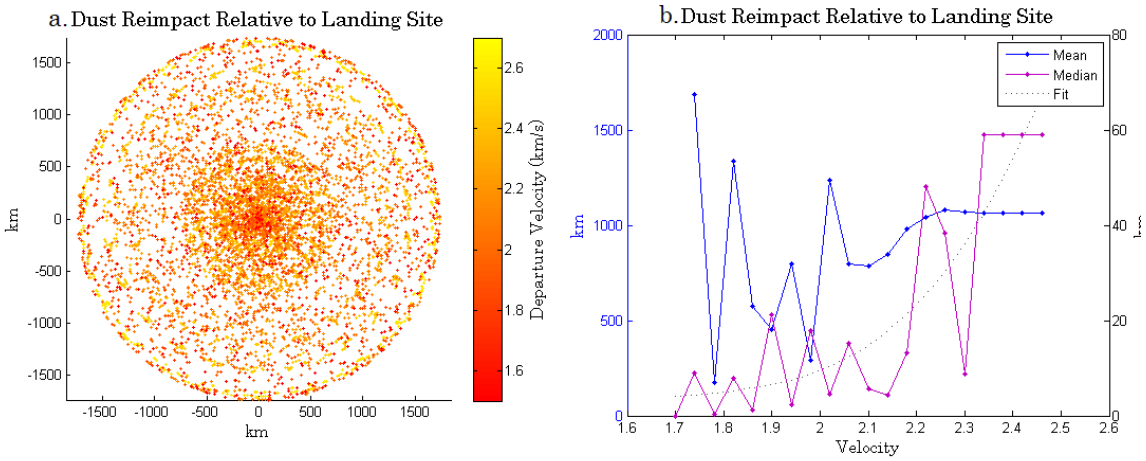

Figure 3. These two plots show the location and distribution as a function of velocity of the particles relative to the landing site. In the first plot, it can be see that the distribution is seemingly random, with particles from across the EVD spectrum reimpacting the surface near the landing site, but also all across the lunar surface.

$$L_I(r) = 8r^{-1.9} \tag{6}$$

Such that at 1 km, an unprotected base might expect as many as 8 impacts per landing, each with a kinetic energy of ∼23.5 J. At 5 km, one would expect a 37 % chance of impact, at 10 km, that falls off to a 10 % chance of impact for base of the same size and so on. Thus, the question of risk turns to a question of durability and materials. It is not a question of *if* an impact will occur, but how many impacts and how the vehicle or space suit handles it.

Scaling this to something in the regime of what would be expected for Artemis, a 40 t lander is expected to generate as much as 6,917 kg of dust between 1.7 km s^{-1} and 2.3 km s^{-1}. Performing the same operation that was described above, this would result in around 150,000 particles. Scaling the coefficient in Eq. 6 to 18 to match the increased particles results in 1,800 %, 84 %, and 22 % chance of impact at 1 km, 5 km, and 10 km respectively.

Using a third case of a 100 t lander generating approximately 286,000 particles, the coefficient increases to ∼34. Using landers of 5 t, 60 t, and 80 t to gather more data points, the coefficient can then be modeled as a function of lander mass and the formula generalized to:

$$L_I(r) = (-0.00085M^2_{\text{Lander}} + 0.39M_{\text{Lander}} + 3.9)r^{-1.9} \tag{7}$$

where M_{Lander} is again the lander mass in tonnes. Due to the nature of the transformation between displaced mass and particle size, it was observed that for extremely small landers (less than 5 t) and extremely large landers (greater than 100 t) the curve is not linear and thus a quadratic fit was used. This is a simple fit and a rough estimation that is expected to be refined in future work.

Risk to Gateway & Orbital Infrastructure

No individual, simulated particle crossed within the Gateway sphere of influence. However, the particles themselves could be thought of as density fields as simulating each individual sub-micron

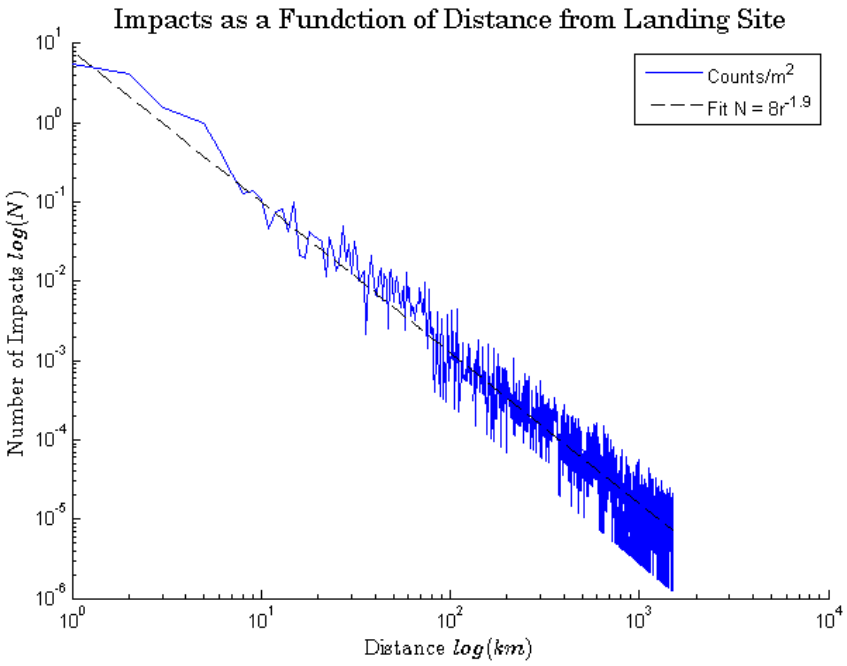

Figure 4. A log-log plot of the number of impacts as a function of distance from the landing site.

particle is impractical. By using the information from Table 1 and combining it with the mass distribution as a function of velocity in Eq. (2), we can estimate how much dust remains in orbit and where it is expected to be at the time of Gateway's first pass after landing. As has been determined above, the vast majority of particles are both extremely small and thus carried away by the solar wind and electric field. Of the $\sim$12 % that remain, $\sim$90 % reimpact the surface. Higher velocity dust may yet remain that poses a hazard, yet dust at these velocities are likewise expected to be increasingly less massive and thus more likely to be carried away into heliocentric space.

Looking strictly at the 10 % of dust that remains and may yet pose a hazard to Gateway, the density of dust can be approximated as particles per cubic kilometer. Kepler's Second Law can be used to estimate the particles at any given point as they sweep out equal areas in equal time, using the Moon as a focal point. The initial velocity of the particle will determine the ellipticity of the orbit, and thus it can be reasoned that the density at perilune will be about the same as that at apolune. Further complicating matters is the time-dependent nature of the dust, which has different periods based, again, on their initial velocity. However, we can perform a rough estimate given what we know about the periods of the dust and the nominal orbit of Gateway.

The dust that poses the greatest hazard to Gateway are those particles which spend the most amount of time near the Gateway's perilune of 3,000 km. This places the threshold of dust initial velocity at $v = \sqrt{\mu(\frac{2}{r} - \frac{1}{a})} = 1.9\,\mathrm{km\,s^{-1}}$. Velocities greater than this spend negligible time within this domain, having periods greater than 2.8 hours and passing twice briefly per orbit within the domain of the Gateway's orbit before eventually leaving the lunar gravity well or reimpacting the surface.

From previous estimates, the total number of particles that remain in orbit is no less than $\sim$6,500 particles for a 10 t lander, the vast majority of which are on the order of 10 µm or smaller. Assuming

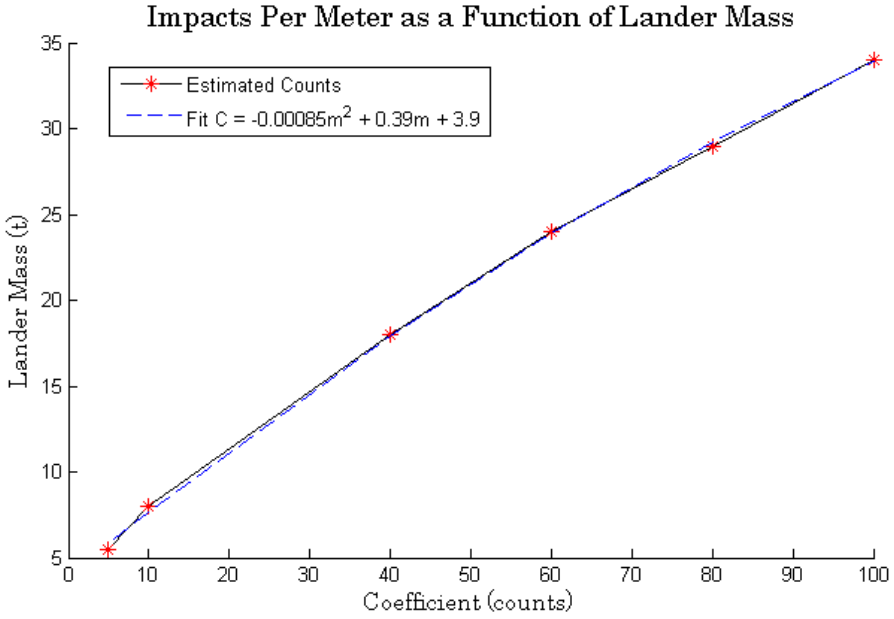

Figure 5. The fit performed based on the log-log data in Fig. 6.

a uniform distribution of these particles over the volume of space occupied by the largest ellipsoid from the 2.3 km s^{-1} minus the smallest ellipsoid occupied by the 1.7 km s^{-1} particles, the total volume in which the particles reside is 3.88418 $\times$ 10^{11} km^3 - 2.46577 $\times$ 10^{10} km^3 = 3.63760 $\times$ 10^{11} km^3, meaning that the estimated number density of particles is 1.7869 $\times$ 10^{-8} km^{-3} when assuming uniform distribution.

CONCLUSION & FUTURE WORK

Based on previous estimates from experimental data, this work has simulated the trajectories of particles between 10 µm and 0.01 m ejected from the south pole by lander plumes between 1.5 km s^{-1} and 2.7 km s^{-1} to determine the possible impact to orbital and surface infrastructure. By including simplified models of electric and magnetic fields in the lunar and orbital environment, it is shown that the impact of particles much smaller than 10 µm is negligible as these particles are greatly influenced by the charged environment and are carried away by the solar wind. The amount of regolith dust that remains is ~12 % of the total ejected as the majority is expected to be very fine. Of that, ~90 % reimpacts the surface preferentially near the landing site, and falling off exponentially in the radial direction. Based on these simulations, a simple approximation is developed to model the likelihood of an impact as a function of distance from the landing site.

Concerns about the reimpacting dust have been shown to have been justified, and further consideration should be given in the future to the construction of landing pads on the Moon to mitigate the spread of fine regolith. However, concerns by the authors and others regarding the safety of the Deep Space Gateway have thus far been shown to be unwarranted. The low amount of fine debris that remain in orbit during Gateway's first pass after landing has a particle number density of approximately 1.7869 $\times$ 10^{-8} km^{-3}.

The model and risk assessment from this work is not intended to be the final word. Far from it,

it is a first past at understanding a large parameter space and extremely dynamic environment that has only begun to be explored. The immediate focus of future work is the near-surface charged environment, which is very dependent on the presence of sunlight and shadow, and the effect of the Earth's magnetotail on the particles in question. Following this, the domain encompassed by the simulation will be expanded to encompass both lower and higher velocities as well as a higher-fidelity simulation.

In addition, there is a vast array of mathematical tools that can be applied to better understand the trends and behavior of the dust in orbit as a function of various phenomena. The development of CFD tools that are effective at simulating plumes in a vacuum currently in development can lead to greater accuracy in generating initial conditions for this kind of high-velocity simulation. Particle-particle interactions that have not been considered in this simulation may also play a factor in the behavior of high-velocity plume ejecta in orbit and near the surface.

Finally, understanding the behavior of impacts of these fine particles both at the surface and on spacecraft can lead to a greater understanding of the necessary steps needed to mitigate mission risk. Although an average kinetic energy of around 23.5 J per reimpacting particle has been determined, the potential for damage has not. Future work also intends to investigate the potential repercussions from extended exposure to these kinds of impacts.

ACKNOWLEDGEMENTS

This work was supported by the NASA Pathways Program. Special thanks to Ben Asher of a.i. Solutions for his assistance in troubleshooting challenges with FreeFlyer and to Adrienne (Addie) Dove of the University of Central Florida for her guidance in understanding the electromagnetic properties of the lunar and near-lunar environment.

REFERENCES

[1] Grün, E., Horanyi, M., & Sternovsky, Z. 2011, Planetary and Space Science, 59, 1672

[2] Calle, C. I. 2017. Electrostatic Phenomena on Planetary Surfaces. Morgan & Claypool Publishers. https://doi.org/10.1088/978-1-6817-4477-3

[3] Rennilson, J. J. & Criswell, D. R. 1974, Moon, 10, 121

[4] Glenar, D. A., Stubbs, T. J., McCoy, J. E., et al. 2011, Planetary and Space Science, 59, 1695

[5] Iglseder, H., Uesugi, K., & Svedhem, H. 1996, Advances in Space Research, 17, 177

[6] Horányi, M., Sternovsky, Z., Lankton, M., et al. 2014, Space Science Reviews, 185, 93

[7] Horányi, M., Szalay, J. R., Kempf, S., et al. (2015). A permanent, asymmetric dust cloud around the moon. Nature, 522, 324-236.

[8] Stubbs, T. J., Vondrak, R. R., & Farrell, W. M. 2007, Dust in Planetary Systems, 643, 239

[9] Wittal, M. M., Powers, R.J (2019). AIAA/AAS Astrodynamics Specialist Conference 19-616

[10] Stubbs, T. J., J. S. Halekas, W. Farrell, and R. Vondrak. 2007. "Lunar surface charging: a global perspective using Lunar Prospector data." Proc Dust Plan Systems, SP-643: 181–184.

[11] Colwell, J. E., Batiste, S., Horányi, M., et al. 2007, Reviews of Geophysics, 45, RG2006

[12] Vaverka, J., Richterová, I., Pavlů, J., et al. 2016, The Astrophysical Journal, 825, 133

[13] Lu, J., Fujii, S., Yasuda, M., & Matsusaka, S. (2020). Analysis of wall fouling and electrostatic charging in gas-solid fluidized beds. Advanced Powder Technology. 10.1016/j.apt.2020.06.034.

[14] Immer, C. D., J. E. Lane, P. T. Metzger, and S. Clements. 2011. "Apollo Video Photogrammetry Estimation of Plume Impingement Effects." Icarus, 214, 46–52.

[15] Metzger, Philip T. 2020. Quantifying Engine Exhaust Ejecta from Landing Large Spacecraft on the Moon," NASA Exploration Science Forum, July 8-10. https://dl.airtable.com/.attachments/d902552c6a4221202134e4629da44416/680f71a7/nesf2020-Metzger-Plume20Ejecta20of20Lunar20Landers.pdf

[16] Housen, K.R., & Holsapple, K.A. (2011). ”Ejecta from impact craters”. Icarus 211 856-875. doi: 10.1016/j.icarus.2010.09.017

[17] Artemieva, N.A. & Shuvalov, V.V.(2008). ”Numerical Simulation of High-Velocity Impact Ejecta Following Falls of Comets and Asteroids onto the Moon”. Solar System Research 2008, vol. 42, No. 4, pp. 329-334. doi:10.1134/S0038094608040059

[18] Lane, J. E., and P. T. Metzger. 2012. “Ballistics Model for Particles on a Horizontal Plane in a Vacuum Propelled by a Vertically Impinging Gas Jet.” Particul. Sci. Tech., 30(2), 196-208.

[19] Metzger, P. T., J. Smith, and J. E. Lane. 2011. “Phenomenology of soil erosion due to rocket exhaust on the Moon and the Mauna Kea lunar test site.” J. Geophys. Res. – Planets. 116. E06005.

[20] Xu, X., Xu, Q., Chang, Q., et al. (2019). ARTEMIS Observations of Well-structured Lunar Wake in Subsonic Plasma Flow. The Astrophysics Journal, 881, 76

[21] Gencturk Akay, I., Kaymaz, Z., & Sibeck, D. G. 2019, Journal of Atmospheric and Solar-Terrestrial Physics, 182, 45